Optimum Differentiation of Frontotemporal Lobar Degeneration from Alzheimer Disease Achieved with Cross-Sectional Tau Positron Emission Tomography

Keith A. Josephs, MD, MST, MSc,[1] Nirubol Tosakulwong, BS,[2] Rodolfo G. Gatto, MD, PhD,[1] Stephen D. Weigand, MS,[2] Farwa Ali, MD,[1] Hugo Botha, MD,[1] Jonathan Graff-Radford, MD,[1] Mary M. Machulda, PhD,[3] Rodolfo Savica, MD, PhD,[1] Christopher G. Schwarz, PhD,[4] Matthew L. Senjem, MS,[4,5] Bradley F. Boeve, MD,[1] Kejal Kantarci, PhD,[4] David T. Jones, MD,[1] Vijay K. Ramanan, MD, PhD,[1] Julie A. Fields, PhD,[3] Ross R. Reichard, MD,[6] Dennis W. Dickson, MD,[7] Ronald C. Petersen, MD, PhD,[1] Clifford R. Jack Jr MD,[4] Val J. Lowe, MD,[4] and Jennifer L. Whitwell, PhD[4]

Objective: This study was undertaken to assess cross-sectional and longitudinal [^{18}F]-flortaucipir positron emission tomography (PET) uptake in pathologically confirmed frontotemporal lobar degeneration (FTLD) and to compare FTLD to cases with high and low levels of Alzheimer disease (AD) neuropathologic changes (ADNC).

Methods: One hundred forty-three participants who had completed at least one flortaucipir PET and had autopsy-confirmed FTLD (n = 52) or high (n = 58) or low ADNC (n = 33) based on Braak neurofibrillary tangle stages 0–IV versus V–VI were included. Flortaucipir standard uptake value ratios (SUVRs) were calculated for 9 regions of interest (ROIs): an FTLD meta-ROI, midbrain, globus pallidum, an AD meta-ROI, entorhinal, inferior temporal, orbitofrontal, precentral, and medial parietal. Linear mixed effects models were used to compare mean baseline SUVRs and annual rate of change in SUVR by group. Sensitivity and specificity to distinguish FTLD from high and low ADNC were calculated.

Results: Baseline uptake in the FTLD meta-ROI, midbrain, and globus pallidus was greater in FTLD than high and low ADNC. No region showed a greater rate of flortaucipir accumulation in FTLD. Baseline uptake in the AD-related regions and orbitofrontal and precentral cortices was greater in high ADNC, and all showed greater rates of accumulation compared to FTLD. Baseline differences were superior to longitudinal rates in differentiating FTLD from high and low ADNC. A simple baseline metric of midbrain/inferior temporal ratio of flortaucipir uptake provided good to excellent differentiation between FTLD and high and low ADNC (sensitivities/specificities = 94%/95% and 71%/70%).

View this article online at wileyonlinelibrary.com. DOI: 10.1002/ana.26479

Received May 5, 2022, and in revised form Aug 10, 2022. Accepted for publication Aug 12, 2022.

Address correspondence to Dr Josephs, Department of Neurology, Behavioral Neurology, and Movement Disorders, Mayo Clinic, College of Medicine and Science, 200 1st Street SW, Rochester, MN 55905. E-mail: josephs.keith@mayo.edu

From the [1]Department of Neurology, Mayo Clinic, Rochester, MN, USA; [2]Department of Quantitative Health Sciences, Mayo Clinic, Rochester, MN, USA; [3]Department of Psychiatry and Psychology, Mayo Clinic, Rochester, MN, USA; [4]Department of Radiology, Mayo Clinic, Rochester, MN, USA; [5]Department of Information Technology, Mayo Clinic, Rochester, MN, USA; [6]Department of Laboratory Medicine and Pathology, Mayo Clinic, Rochester, MN, USA; and [7]Department of Neuroscience (Neurogenetics), Mayo Clinic, Jacksonville, FL, USA

Interpretation: There are cross-sectional and longitudinal differences in flortaucipir uptake between FTLD and high and low ADNC. However, optimum differentiation between FTLD and ADNC was achieved with baseline uptake rather than longitudinal rates.

ANN NEUROL 2022;92:1016–1029

Molecular positron emission tomography (PET) ligands that bind to tau proteins, such as [^{18}F]-flortaucipir,[1] allow the in vivo assessment of the presence and distribution of tau deposition in the brain. Flortaucipir shows excellent binding to the 3R + 4R paired helical filament tau deposited as neurofibrillary tangles (NFTs) in patients with Alzheimer disease (AD).[2–4] Elevated uptake of flortaucipir is observed in patients with Alzheimer dementia,[5,6] and the severity and regional distribution of uptake matches well with underlying Braak NFT stage in AD.[7–10] Furthermore, it has been shown that flortaucipir PET outperforms other neuroimaging modalities in differentiating AD from other non-AD neurodegenerative diseases.[11] Longitudinal studies of flortaucipir have demonstrated increasing uptake over time in patients with Alzheimer dementia,[12,13] although it is unknown how longitudinal changes relate to autopsy findings in AD.

Frontotemporal lobar degeneration (FTLD) is the second most common neurodegenerative disease in patients younger than 65 years.[14] FTLD is an umbrella term that encompasses several different molecular pathologies that target the frontal and temporal lobes, particularly pathologies characterized by the deposition of 4R tau, 3R tau, and TAR DNA-binding protein of 43kDa (TDP-43).[15] The majority of FTLD cases are sporadic, although genetic mutations have been identified.[16] Many different clinical syndromes are associated with FTLD molecular pathology, including those characterized predominantly by impairment of speech and language, and personality and behavioral change, as well as disorders with prominent pyramidal and extrapyramidal motor features. Elevated flortaucipir uptake has been observed in frontotemporal, subcortical, and brainstem regions in the FTLD clinical syndromes,[17–24] including in those associated with underlying 4R tau,[18,20,21] 3R tau,[25] and FTLD-TDP,[17,19,22,26] with longitudinal changes in uptake observed in 2 FTLD clinical syndromes.[18] Cross-sectionally, flortaucipir uptake in FTLD is typically milder than that observed in AD, with uptake observed in a different regional distribution.[18,27,28] It is unknown whether rates of change in flortaucipir differ between FTLD and AD and whether regional distinctions are relevant longitudinally. It is also unknown how cross-sectional uptake compares to longitudinal change across the two diseases. Addressing these knowledge gaps would help answer the question of which approach and associated brain regions are superior and hence, can be utilized as biomarkers to differentiate FTLD from AD.

In this study, we aimed to determine whether regional cross-sectional (baseline) and longitudinal flortaucipir PET findings differ between sporadic FTLD and AD, and how best to differentiate between the two diseases. To achieve our aims, we use autopsy-confirmed cohorts. This allowed us to specifically assess how FTLD compares to cases with high and low probabilities of AD neuropathological changes (ADNC).[29] We hypothesize that in FTLD-specific regions, baseline flortaucipir uptake will be greater in FTLD than in high and low ADNC, that there will be comparable regional rates of uptake over time between FTLD and low ADNC, and that AD-specific regions would best differentiate between high ADNC and FTLD.

Materials and Methods

Participants

To be included in this study, all subjects had to (1) have completed at least one flortaucipir PET scan and (2) have died with an autopsy diagnosis of an FTLD spectrum disease or ADNC (any combination of Braak NFT stages 0–VI and Thal phases 0–5). All FTLD cases also had to have screened negative for a mutation in all 3 major FTLD-associated genes, including *MAPT*, *GRN*, and *C9ORF72*.[16] We chose not to include FTLD participants with genetic mutations, given that some mutations are associated with 3R + 4R Alzheimer type neuropathology and show flortaucipir uptake in the range associated with high ADNC, and hence would confound the results.[30] We identified 147 participants who met our inclusion criteria and excluded 4 patients with low levels of ADNC who had another "primary" pathological diagnosis (3 with multiple system atrophy and 1 with mitochondrial encephalomyopathy, lactic acidosis, and strokelike episodes). All remaining 143 participants had been recruited into an National Institutes of Health-funded study between January 1, 2015 and August 30, 2021. The FTLD participants had all been recruited by the Neurodegenerative Research Group (NRG), and the ADNC participants had been recruited by the NRG, the Mayo Clinic Alzheimer's Disease Research Center, or the Mayo Clinic Study of Aging.

The study was approved by the Mayo Clinic Institutional Review Board, and all participants or their proxies provided written informed consent to participate in this study.

Neuropathology

All 143 participants had died and underwent standard neuropathological examination performed by a board-certified neuropathologist (D.W.D. or R.R.R.) as previously described in detail.[26] Of the 143 participants, 52 met criteria for FTLD[31]

with focal neuronal loss and gliosis affecting frontal and/or temporal lobe, whereas the rest of the cohort did not have features of FTLD but showed varying amounts of ADNC. The majority (n = 46) of the FTLD cohort consisted of cases with tau molecular pathology (FTLD-tau; 44 with 4R tau, 2 with 3R tau),[32] with 6 cases having TDP-43 (ie, FTLD-TDP).[32] For the purpose of this study and guided by the National Institute of Aging–Alzheimer's Association recommendations, we subclassified the 91 ADNC participants into high and low/intermediate (referred to from here onward as low) ADNC groups based on the following Braak NFT stages[33]: low ADNC (n = 33, Braak NFT stage ≤ IV) or high ADNC (n = 58, Braak NFT stage > IV).[29] The criteria used to split the ADNC group were also motivated by our aim to match the low ADNC group to the FTLD group in terms of the Braak NFT stage,[33] because it is well known that some FTLD cases also have NFTs.

Image Acquisition

All 143 participants underwent a structural head magnetic resonance imaging (MRI) and flortaucipir tau-PET scan. Flortaucipir PET scans were acquired using a PET/computed tomography (CT) scanner (GE Medical Systems, Milwaukee, WI) operating in 3-dimensional mode. An intravenous bolus injection of approximately 370MBq (range = 333–407MBq) of flortaucipir was administered, followed by a 20-minute PET acquisition performed 80 minutes after injection. The [^{18}F]-flortaucipir scans consisted of four 5-minute dynamic frames following a low-dose CT transmission scan. Standard corrections were applied. Emission data were reconstructed into a 256 × 256 matrix with a 30cm field of view (in-plane pixel size = 1.17mm). All participants also underwent a 3T head MRI protocol using GE scanners that included a magnetization prepared rapid gradient echo (MPRAGE) sequence (repetition time/echo time/inversion time = 2,300/3/900 milliseconds, flip angle = 8°, 26cm field of view (FOV), 256 × 256 in-plane matrix, phase FOV = 0.94cm, slice thickness = 1.2mm). The MRI scans were performed a median of 1 day from the flortaucipir PET scans.

Image Processing

Baseline Cross-Sectional Measurements. Each PET image was rigidly registered to its corresponding MPRAGE using SPM12 (Welcome Trust Centre for Neuroimaging, London, UK). Using Advanced Normalization Tools, the Mayo Clinic Adult Lifespan Template (MCALT) (https://www.nitrc.org/projects/mcalt/) atlases were propagated to the native MPRAGE space and used to calculate regional PET values in the gray and white matter. Tissue probabilities were determined for each MPRAGE using Unified Segmentation in SPM12, with MCALT tissue priors and settings. Standard uptake value ratios (SUVRs) were created normalizing uptake in each region of interest (ROI) to the cerebellar crus gray matter.[34] Two-compartment partial volume correction (PVC) was applied.

Longitudinal (Change) Measurements. Sixty-three subjects had at least 2 flortaucipir PET scans, with 1 scan failing preprocessing, leaving 62 subjects for longitudinal analyses. We assessed change in tau PET SUVR using a previously published in-house intrasubject cross-time longitudinal pipeline[35] shown to enhance repeatability and effect sizes of change measurements. Briefly, intrasubject MRIs were group-coregistered, and bias fields (intensity inhomogeneity) were harmonized before creating a nonlinear single-subject template (T1-SST) with atlas spatial normalization using Advanced Registration Tools.[35] MRIs were each resampled to this T1-SST space and individually segmented using the same methods as in the cross-sectional pipeline above, to produce tissue probabilities and atlas ROIs. Intrasubject PETs across time were group-coregistered to form a rigid single-subject PET template (PET-SST). A single rigid registration was computed between T1-SST and PET-SST, and this was used to resample all PETs to the space of T1-SST. Two-compartment PVC was applied, and SUVRs were calculated using the atlas ROIs from each PET in T1-SST space. Unlike the cross-sectional pipeline, our SUVR normalization for change measurements used a composite reference region comprised of eroded supratentorial white matter, pons, and whole cerebellum.[35]

Regions of Interest. We analyzed 9 specific ROIs that were selected a priori. First, regional uptake was calculated in 2 meta-ROIs: (1) an FTLD meta-ROI that consisted of 5 subcortical brain regions that have been shown to have elevated flortaucipir uptake in FTLD[18,20] (thalamus, dentate nucleus of cerebellum, globus pallidum, subthalamic nucleus, midbrain) and (2) an AD meta-ROI that consisted of 6 cortical brain regions that typically show elevated flortaucipir uptake in AD (entorhinal cortex, amygdala, parahippocampal, fusiform, inferior temporal, and middle temporal gyri). The FTLD meta-ROI was selected based on previous studies that have found these regions are most affected in autopsy-confirmed FTLD-tau,[26] as well as in clinically diagnosed behavioral variant frontotemporal dementia (bvFTD) cases,[24] where FTLD-TDP pathology would be expected to account for at least 50% of the cases.[36] Previous studies show that the AD meta-ROI cut-point accurately captures within-subject tau signal for longitudinal analysis and has broad dynamic range across the normal to AD spectrum.[12] For each meta-ROI, a weighted average of uptake was calculated across regions. Seven additional regions were also specifically assessed: inferior temporal cortex, entorhinal cortex, precentral cortex, medial parietal cortex (posterior cingulate + precuneus), midbrain, globus pallidum, and orbitofrontal cortex. The precentral cortex and orbitofrontal cortex were selected due to their involvement in both FTLD and AD.[20,21,24,37]

Statistical Analyses

We compared regional mean baseline flortaucipir SUVR values across neuropathological diagnosis groups by fitting a linear regression model in each ROI. These models used baseline log-transformed SUVR from the cross-sectional pipeline as the response and neuropathological diagnosis group as the primary predictor. Age, years from baseline scan to death, and presence/absence of vascular disease (small/large/ischemic/hemorrhagic infarctions) identified on MRI were included as covariates. We also used SUVR values from the longitudinal pipeline described above to compare mean rates of change across groups by fitting linear mixed effects models in each ROI. These mixed models

were fit only among those with at least 2 PET scans. We used log SUVR as the response and included the following fixed effects: age at first tau PET, years from baseline scan to death, presence/absence of vascular disease (any infarctions) on MRI, neuropathological diagnosis group, time from first tau PET, and a group-by-time interaction. Each model also included participant-specific random intercepts and slopes. We used a log transformation in our regression models to address right skew, to account for the tendency for greater intrinsic variability at higher SUVR values, and so that regression coefficients could be interpreted as percentage differences after the back-transformation $100 \times (\exp[\beta] - 1)$. The percentage difference interpretation is particularly convenient because it allows for direct comparisons between groups and across ROIs. We used the stan_lmer function in the rstanarm package with R version 4.0.3 to fit mixed effects models using a Bayesian framework with weakly informative priors.[38] We also performed a sensitivity analysis by omitting the 6 FTLD-TDP participants and performing the linear regression and mixed model analyses described above.

We also performed an area under the receiver operating curve (AUROC) analysis using participants' first tau PET and using participants' annual rate of change obtained from the longitudinal pipeline and estimated via a least square fit to everyone's log SUVR values over time. A cutoff minimizing the difference between sensitivity and specificity was used to characterize the diagnostic properties of baseline and annual change in tau PET in each ROI. We used a chi-squared test among the subset of participants with serial PET scans to test for any significant difference between baseline AUROC and annual change in AUROC for the AD meta-ROI and among all participants to test for any significant difference between the ratios of midbrain/inferior temporal and FTLD meta-ROI/AD meta-ROI, and the best ROI that differentiated between groups for each comparison. The ratio of midbrain/inferior temporal was motivated by our goal of generating a simple variable that could be easily calculated, yet potentially be superior to any individual ROI, given that it takes into account an ROI with prominent increased uptake in FTLD but less so in ADNC (midbrain) divided by an ROI with prominent increased uptake in ADNC but less so in FTLD (inferior temporal).

Results

Demographic and Clinical Differences between the 3 Groups

There were significant differences in demographic and clinical characteristics between the 3 groups (Table 1). Differences were observed in sex, with the lowest frequency of females observed in low ADNC, and in *APOE* ε4 frequency, with the lowest frequency observed in FTLD. The FTLD group was the youngest at baseline scan and death. Both FTLD and high ADNC groups were more cognitively and functionally impaired than the low ADNC group. Antemortem clinical diagnoses differed between the 3 groups, as expected, with the majority of the FTLD group having a frontotemporal lobar degeneration syndrome (87%), the majority of the high ADNC group having mild cognitive impairment/Alzheimer dementia (86%), and about half of the participants in the low ADNC group being cognitively unimpaired (52%). Frontotemporal lobar degeneration syndromes in the FTLD group were split almost equally between a cognitive or behavioral dominant presentation (bvFTD, agrammatic/nonfluent primary progressive aphasia, or semantic primary progressive aphasia, n = 23) and a motor dominant presentation (progressive supranuclear palsy or corticobasal syndrome, n = 22), covering the spectrum of FTLD-related clinical syndromes.[39] Pathologically, the Braak NFT stage, Thal phase, and presence of Lewy bodies also differed across groups, although the FTLD and low ADNC groups had relatively similar median Braak NFT stages as per study design.

Sixty-two participants had >1 flortaucipir PET scan (Table 2), with 36 participants having 2 serial scans, 18 having 3 serial scans, 8 having 4 serial scans, and 1 having 5 serial scans. There were similar differences and/or trends in demographic and clinical features across the 3 groups in the longitudinal cohort as in the larger cross-sectional cohort. Of note, participants with low ADNC in the longitudinal cohort were more functionally impaired as a group and less likely to be cognitively unimpaired (33%) compared to those in the cross-sectional cohort (52%).

Flortaucipir Differences between the 3 Groups

Serial flortaucipir PET SUVRs in the cohort for all 9 ROIs is shown in Figure 1. There was significant overlap observed across groups for the FTLD meta-ROI, midbrain, and pallidum. For the remaining 6 ROIs, more separation was observed with the high ADNC group, showing greater SUVRs compared to the low ADNC and FTLD groups. This was particularly striking for the AD meta-ROI, and the inferior temporal and medial parietal cortices.

The results of the mixed effects analysis are shown in Table 3 and Figure 2. The FTLD group had greater baseline flortaucipir uptake in the FTLD meta-ROI, midbrain, and globus pallidus compared to both the high and low ADNC groups. On the other hand, the FTLD group and the low ADNC group showed lower baseline flortaucipir uptake in the AD meta-ROI, entorhinal cortex, inferior temporal cortex, orbitofrontal cortex, precentral cortex, and medial parietal cortex compared to the high ADNC group. There was no difference in flortaucipir uptake in these 6 regions between low ADNC and FTLD.

The FTLD group showed lower rates of longitudinal flortaucipir change in the AD meta-ROI, inferior temporal cortex, orbitofrontal cortex, and precentral cortex compared to the high ADNC group (see Table 3 and Fig 2).

TABLE 1. Demographic and Clinical Characteristics of All Participants

Characteristic	Low AD, n = 33	FTLD, n = 52	High AD, n = 58	Overall *p*
Female, n (%)	6 (18%)	21 (40%)	27 (47%)	0.02[a]
APOE ε4 carrier, n (%)	15 (47%)	10 (21%)	31 (57%)	<0.001[b]
Education, yr	14 (12–17)	16 (12–16)	14 (12–16)	0.66
Age at onset, yr	67 (64–82)	64 (56–71)	65 (57–76)	0.12
Age at baseline tau, yr	79 (71–85)	70 (63–76)	74 (65–83)	0.004[b]
Age at death, yr	81 (76–88)	74 (66–78)	78 (68–87)	0.001[b]
Serial tau, n (%)	12 (36%)	23 (45%)	27 (47%)	0.65
Vascular disease present at baseline, n (%)	9 (27%)	7 (13%)	12 (21%)	0.30
Braak neurofibrillary tangle stage	3.0 (2.0–4.0)	2.5 (1.0–3.0)	6.0 (5.0–6.0)	<0.001[c]
Thal phase	3.0 (1.0–3.2)	0.0 (0.0–2.0)	5.0 (4.0–5.0)	<0.001[d]
LBD present, n (%)	19 (61%)	3 (14%)	23 (41%)	0.002[b]
LBD stage, n (%)				0.22
Brainstem-predominant	4 (21%)	1 (33%)	1 (5%)	
Limbic or amygdala-predominant	5 (26%)	1 (33%)	11 (52%)	
Neocortical [diffuse]	10 (53%)	1 (33%)	9 (43%)	
MMSE	27 (24–28)	23 (17–25)	20 (14–22)	<0.001[a]
CDR-SB	0.8 (0.0–6.2)	8.0 (1.9–11.8)	7.0 (3.0–11.0)	0.005[e]
Last known clinical diagnosis, n (%)				<0.001[d]
Normal	17 (52%)	0 (0%)	2 (3%)	
MCI/AD	8 (24%)	6 (12%)	50 (86%)	
FTD	0 (0%)	45 (87%)	2 (3%)	
DLB	8 (24%)	1 (2%)	4 (7%)	

Data shown are as median (range) or n (%). For continuous variables, *p* values are from Kruskal–Wallis test, followed by Wilcoxon rank sum tests. For categorical variables, *p* values are from Fisher exact test.
[a]Low ADNC is statistically different from high ADNC/FTLD.
[b]FTLD is statistically different from low/high ADNC.
[c]High ADNC is statistically different from low ADNC/FTLD.
[d]All groups are statistically different from each other.
[e]Low ADNC is statistically different from high ADNC.
AD = Alzheimer disease; ADNC = AD neuropathological changes; *APOE* = apolipoprotein, CDR-SB = Clinical Dementia Rating Scale–Sum of Boxes; DLB = dementia with Lewy bodies, FTD = frontotemporal dementia; FTLD = frontotemporal lobar degeneration; LBD = Lewy body disease; MCI = mild cognitive impairment; MMSE = Mini-Mental State Examination.

The results of the sensitivity analysis that excluded the FTLD-TDP cases, and hence compared FTLD-tau to high and low ADNC (Fig 3), did not differ from those that included all FTLD participants (Fig 2).

Sensitivity and Specificity of the 8 ROIs

Sensitivity and specificity data are shown in Tables 4 to 6. The baseline AD meta-ROI, entorhinal cortex, inferior temporal cortex, midbrain/inferior temporal ratio, and FTLD meta-ROI/AD meta-ROI ratio SUVRs all had excellent AUROCs of ≥0.90, with high sensitivity and specificity to distinguish between high ADNC and both FTLD and low ADNC. The baseline FTLD meta-ROI, midbrain, precentral cortex, midbrain/inferior temporal ratio, and FTLD meta-ROI/AD meta-ROI ratio SUVRs had acceptable AUROCs (>0.75) to differentiate FTLD

TABLE 2. Demographic and Clinical Characteristics of All Participants in the Longitudinal Cohort

Characteristic	Low AD, n = 12	FTLD, n = 23	High AD, n = 27	Overall *p*
Female, n (%)	3 (25%)	6 (26%)	13 (48%)	0.23
APOE ε4 carrier, n (%)	5 (42%)	6 (27%)	15 (58%)	0.10
Education, yr	15 (12–17)	16 (16–18)	14 (12–16)	0.15
Age at onset, yr	67 (64–73)	64 (57–68)	63 (56–73)	0.42
Age at baseline tau, yr	79 (72–85)	70 (64–76)	77 (72–81)	0.04[a]
Age at death, yr	82 (76–87)	75 (68–78)	81 (76–86)	0.02[a]
Follow-up time, yr	1.4 (1.1–2.5)	1.4 (1.0–2.4)	1.4 (1.1–2.2)	0.96
Vascular disease present at baseline, n (%)	2 (17%)	3 (13%)	9 (33%)	0.23
Braak neurofibrillary tangle stage	3.0 (2.0–3.2)	2.0 (1.0–3.0)	6.0 (5.0–6.0)	<0.001[b]
Thal phase	3.0 (0.8–4.0)	2.0 (0.0–2.5)	5.0 (4.0–5.0)	<0.001[c]
LBD present, n (%)	10 (91%)	2 (15%)	11 (44%)	<0.001[d]
LBD stage, n (%)				0.73
Brainstem-predominant	2 (20%)	0 (0%)	1 (10%)	
Limbic or amygdala-predominant	2 (20%)	1 (50%)	5 (50%)	
Neocortical [diffuse]	6 (60%)	1 (50%)	4 (40%)	
MMSE	26 (22–27)	24 (16–26)	20 (14–22)	0.01[e]
CDR-SB	4.8 (2.5–7.9)	8.0 (1.0–12.0)	8.5 (4.5–11.0)	0.46
Last known clinical diagnosis, n (%)				<0.001[c]
Normal	4 (33%)	0 (0%)	1 (4%)	
MCI/AD	3 (25%)	5 (22%)	22 (81%)	
FTD	0 (0%)	17 (74%)	1 (4%)	
DLB	5 (42%)	1 (4%)	3 (11%)	

Data shown are median (range) or n (%). For continuous variables, *p* values are from Kruskal–Wallis test, followed by Wilcoxon rank sum tests. For categorical variables, *p* values are from Fisher exact test.
[a]FTLD is statistically different from low/high ADNC.
[b]High ADNC is statistically different from low ADNC/FTLD.
[c]All groups are statistically different from each other.
[d]Low ADNC is statistically different from high ADNC/FTLD.
[e]Low ADNC is statistically different from high ADNC.
AD = Alzheimer disease; ADNC = AD neuropathological changes; *APOE* = apolipoprotein, CDR-SB = Clinical Dementia Rating Scale–Sum of Boxes; DLB = dementia with Lewy bodies, FTD = frontotemporal dementia; FTLD = frontotemporal lobar degeneration; LBD = Lewy body disease; MCI = mild cognitive impairment; MMSE = Mini-Mental State Examination.

from low ADNC, with 71% sensitivity and 70% specificity achieved for the midbrain/inferior temporal ratio. The AUROCs to differentiate between groups using rates of flortaucipir change were not as good as baseline measures. Only the FTLD meta-ROI/AD meta-ROI ratio SUVR achieved an AUROC of >0.75 to differentiate between high ADNC and FTLD, with 65% sensitivity and 67% specificity. The only ROI to have an AUROC > 0.75 to differentiate between FTLD and low ADNC was the FTLD meta-ROI, with 65% sensitivity and 67% specificity. The only ROI to have an excellent AUROC to differentiate between high ADNC and low ADNC was the precentral ROI (AUROC = 0.84), which had 70% sensitivity and 67% specificity.

Among the 62 participants who had completed longitudinal flortaucipir PET scanning, the cross-sectional AD

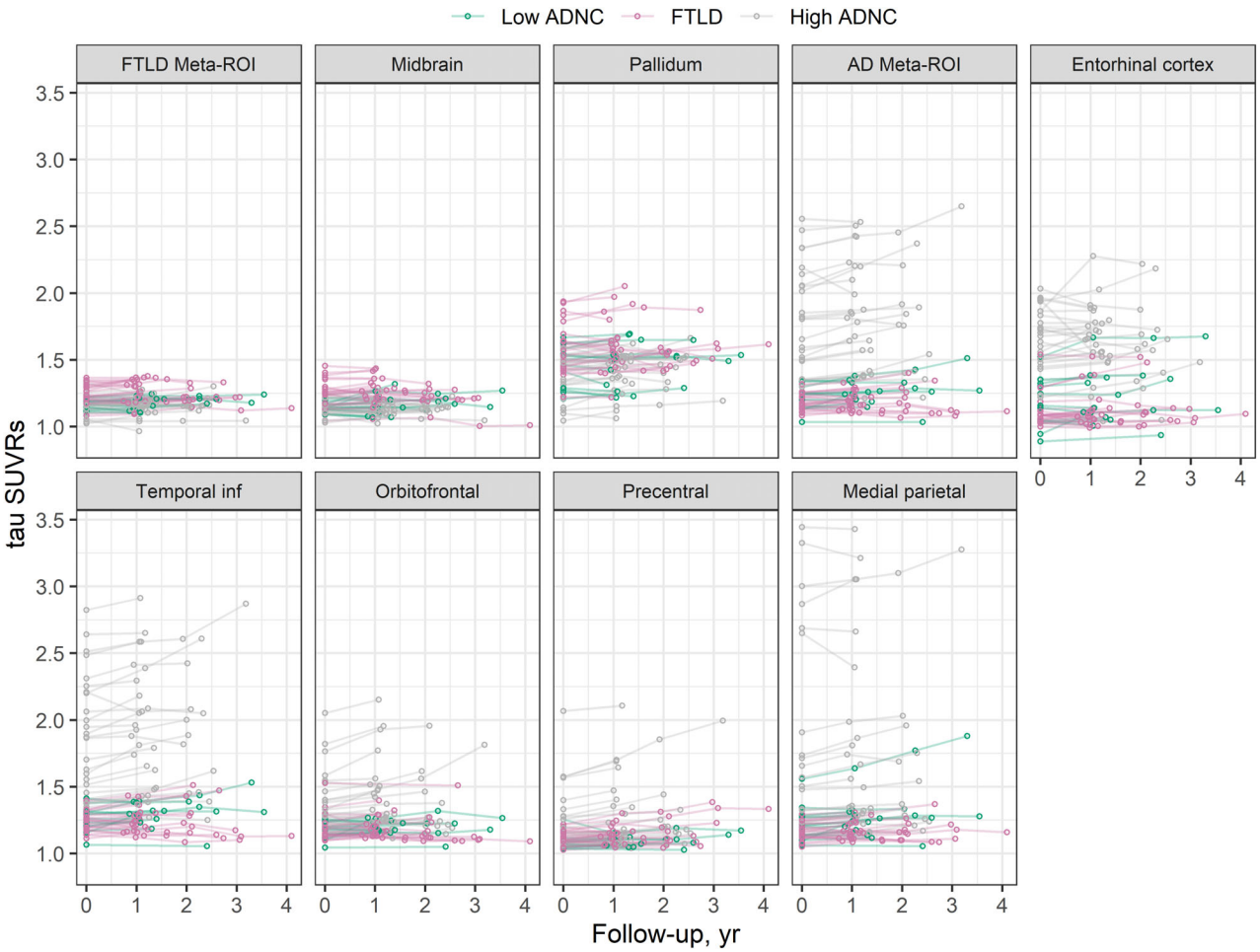

FIGURE 1: Spaghetti plots of flortaucipir standard uptake value ratios (SUVRs) by diagnosis. Quantitative longitudinal representation of flortaucipir SUVR in the 8 different region of interests (ROIs) from 3 study groups is shown (low Alzheimer disease [AD] neuropathological changes [ADNC], high ADNC, and frontotemporal lobar degeneration [FTLD]). inf = inferior.

meta-ROI AUROC was significantly greater than the longitudinal AD meta-ROI AUROC for differentiating FTLD and high ADNC (0.90 vs 0.73, $\chi^2[1\ df] = 4.5$, $p = 0.03$).

Among the 143 participants who had completed baseline flortaucipir PET scanning, the AUROC for the midbrain/inferior temporal ratio was greater than the AUROC for the AD meta-ROI for differentiating FTLD and high ADNC (see Table 4; 0.99 vs 0.94, $\chi^2[1\ df] = 5.4$, $p = 0.02$), but no differences in AUROCs were observed between the midbrain/inferior temporal ratio and the FTLD meta-ROI for differentiating FTLD and low ADNC (see Table 5; 0.80 vs 0.77, $\chi^2[1\ df] = 0.3$, $p = 0.60$) or the AD meta-ROI for differentiating high ADNC and low ADNC (see Table 6; 0.94 vs 0.93, $\chi^2[1\ df] = 0.3$, $p = 0.60$).

Flortaucipir Comparison between FTLD Subgroups

As a secondary analysis, we stratified the FTLD group by molecular pathology, that is, FTLD-tau (n = 46) versus FTLD-TDP (n = 6). Both groups had a similar frequency of female participants (FTLD-tau, 39%; FTLD-TDP, 50%), and similar *APOE* ε4 allele frequency (FTLD-tau, 21%; FTLD-TDP, 17%). Median age at onset in the FTLD-tau subgroup was 64 years (interquartile range = 57–72) compared to 57 years (range = 56–57) in FTLD-TDP. The flortaucipir baseline SUVRs and rates of change for the FTLD-tau and FTLD-TDP cases are shown in Figure 4. There was a lot of overlap between groups for baseline and rates of change, with little evidence for any one ROI being strikingly different between the two groups except for possibly medial parietal cortex.

Interpretation

This study demonstrates that [^{18}F]-flortaucipir PET has a specific regional pattern of uptake in subcortical structures in FTLD and that uptake in these regions is greater in FTLD than both high and low ADNC, although less difference was observed longitudinally. Excellent differentiation of FTLD and high ADNC is obtained with baseline uptake in AD-related regions, which are more affected in

TABLE 3. Percent Estimated Differences between Low ADNC/FTLD and High ADNC

ROI	Low ADNC vs High ADNC	FTLD vs High ADNC	Low ADNC vs FTLD
Baseline			
FTLD meta-ROI	−4% (−8% to 0.1%)	4% (1% to 8%)	−8% (−12% to −4%)
Midbrain	−4% (−8% to 0.1%)	6% (2% to 10%)	−9% (−13% to −5%)
Pallidum	−4% (−9% to 1%)	9% (4% to 15%)	−12% (−17% to −7%)
AD meta-ROI	−34% (−39% to −29%)	−37% (−42% to −33%)	5% (−3% to 14%)
Entorhinal cortex	−32% (−36% to −27%)	−32% (−37% to −28%)	1% (−6% to 9%)
Temporal inf	−36% (−41% to −30%)	−39% (−43% to −34%)	4% (−4% to 14%)
Orbitofrontal	−20% (−26% to −14%)	−20% (−25% to −14%)	−1% (−8% to 7%)
Precentral	−19% (−24% to −13%)	−15% (−20% to −9%)	−5% (−11% to 3%)
Medial parietal	−33% (−40% to −26%)	−39% (−45% to −33%)	10% (−1% to 23%)
Rates			
FTLD meta-ROI	−0.1% (−1% to 1%)	0.7% (−0.2% to 2%)	−1% (−2% to 0.2%)
Midbrain	1% (−1% to 2%)	0.5% (−0.6% to 2%)	0.1% (−1% to 2%)
Pallidum	−1% (−2% to 1%)	0.1% (−1% to 1%)	−1% (−2% to 1%)
AD meta-ROI	−1% (−3% to 0.3%)	−2% (−3% to −1%)	1% (−1% to 3%)
Entorhinal cortex	1% (−2% to 3%)	−1% (−3% to 2%)	2% (−1% to 5%)
Temporal inf	−1% (−3% to 1%)	−2% (−4% to −1%)	1% (−1% to 3%)
Orbitofrontal	−1% (−3% to 1%)	−2% (−4% to −1%)	1% (−1% to 3%)
Precentral	−3% (−4% to −1%)	−2% (−3% to −1%)	−1% (−3% to 0.4%)
Medial parietal	0.4% (−1% to 2%)	−1% (−2% to 0.4%)	2% (0.01% to 3%)

Estimates shown for baseline difference are point estimates and 95% confidence intervals from linear regression models. Estimates shown for rate differences are point estimates and 95% confidence intervals for the posterior distribution from linear mixed models fit within a Bayesian framework.
AD = Alzheimer disease; ADNC = AD neuropathologic changes; FTLD = frontotemporal lobar degeneration; inf = inferior; ROI = region of interest.

high ADNC, although optimum differentiation is obtained with a simple ratio of midbrain/inferior temporal SUVR.

The FTLD group showed elevated baseline uptake in the midbrain, pallidum, and an FTLD meta-ROI that also included the dentate nucleus of the cerebellum, subthalamic nucleus, and thalamus. Elevated tau PET uptake has previously been observed in these regions, except for the FTLD meta-ROI, in clinical cohorts of patients suspected of having underlying FTLD, such as those with bvFTD[24] and those with motor predominant syndromes,[18,20,21] and in autopsy-confirmed FTLD-tau patients.[26] We extend these findings by showing that uptake in these regions, including an FTLD meta-ROI, was greater than that observed in participants with both low- and high-probability ADNC, thereby demonstrating specificity for FTLD. Elevated tau PET uptake has also been previously observed in precentral cortex and frontal cortex in clinical FTLD cohorts,[20,24] although our study shows that these regions are strikingly more affected in high ADNC compared to FTLD. As expected, our AD-related ROIs, including the AD meta-ROI, entorhinal cortex, inferior temporal cortex, and medial parietal cortex, also showed greater uptake in high ADNC compared to FTLD. These AD-related ROIs showed excellent AUROC values to differentiate FTLD from high AD, with sensitivity and specificity values comparable to those previously observed to differentiate clinically diagnosed cohorts of AD from non-AD dementias.[11] The FTLD meta-ROI showed only moderate sensitivity/specificity

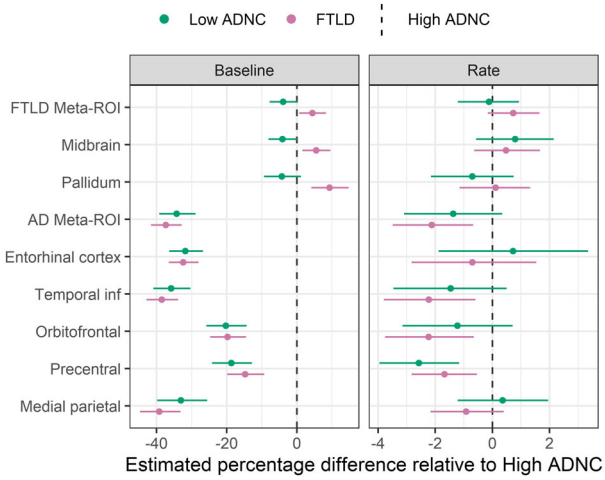

FIGURE 2: Plots of percent estimated differences between low Alzheimer disease (AD) neuropathological changes (ADNC)/frontotemporal lobar degeneration (FTLD) versus high ADNC groups. Comparative baseline and flortaucipir positron emission tomography rates for the low ADNC and FTLD groups are compared to the high ADNC group (high ADNC is the reference group represented by the *dashed line*). Estimates shown for baseline difference are point estimates and 95% confidence intervals from linear regression models. Estimates shown for rate differences are point estimates and 95% confidence intervals for the posterior distribution from linear mixed models fit within a Bayesian framework. Data are shown both without (left panel) and with (right panel) partial volume correction. inf = inferior, ROI = region of interest.

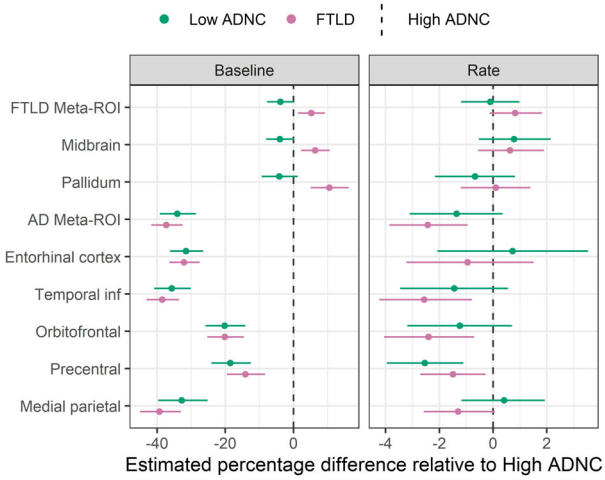

FIGURE 3: Plots of percent estimated differences between low Alzheimer disease [AD] neuropathological changes (ADNC)/frontotemporal lobar degeneration (FTLD)-tau versus high ADNC groups. Comparative baseline and flortaucipir positron emission tomography rates for the low ADNC and FTLD-tau groups are compared to the high ADNC group (high ADNC is the reference group represented by the *dashed line*), removing the FTLD-TAR DNA binding protein 43 cases. Estimates shown for baseline difference are point estimates and 95% confidence intervals from linear regression models. Estimates shown for rate differences are point estimates and 95% confidence intervals for the posterior distribution from linear mixed models fit within a Bayesian framework. Data are shown both without (left panel) and with (right panel) partial volume correction. inf = inferior; ROI = region of interest.

values to differentiate FTLD from high ADNC but provided good differentiation of FTLD from low ADNC. This is intuitive if we consider that the Braak NFT stages were similar in FTLD and low ADNC, and therefore AD-related regions would be expected to do poorly at separating the groups, with FTLD-related regions being better. The reason the FTLD meta-ROI was better able to differentiate FTLD from low ADNC compared to high ADNC may be that the FTLD-related regions are more likely to have higher NFT burden in high ADNC compared to low ADNC. Flortaucipir metrics, therefore, have potential clinical utility to differentiate sporadic FTLD patients from both low and high ADNC patients.

Longitudinal differences were also observed between FTLD and high ADNC, with the high ADNC participants showing greater rates of tau accumulation in all temporal and cortical regions, except the entorhinal and medial parietal cortices. Increased rates of tau accumulation in the AD meta-ROI and lateral temporal regions have also been observed in clinically diagnosed Alzheimer dementia patients compared to cognitively unimpaired controls.[12,40] The lack of difference in the entorhinal cortex is interesting and could be because entorhinal tau deposition occurs early in FTLD patients. The entorhinal cortex is one of the first regions to show tau uptake in preclinical AD,[6,41,42] and 19% of the FTLD participants had a Braak stage of IV and, hence, could have enough tau deposition in the entorhinal cortex to be detected with flortaucipir PET.[7,10,26] It is also possible that tau deposition in the entorhinal cortex in the high ADNC participants has somewhat plateaued, given its lower rates of tau accumulation compared to other temporal and cortical regions. The concept that tau deposition measured by flortaucipir PET reaches a plateau in the earliest affected regions but continues to spread into later affected regions has previously been hypothesized.[37,43,44] The lack of a difference in rate for the medial parietal cortex is less clear. It is intriguing that by removing the 6 FTLD-TDP participants, the difference in medial parietal rates almost becomes significant. Although longitudinal differences were observed between high ADNC and FTLD, the effect sizes to differentiate these pathologies were much lower than those observed for baseline uptake in the AD-related regions. This may be due in part to the large degree of variability observed in the longitudinal rate estimates likely resulting from measurement noise, artifacts, and potentially off-target uptake,[45] or may suggest that

TABLE 4. AUROC, Sensitivity, and Specificity Data Comparing FTLD and High ADNC Using Baseline and Rates of Change in Flortaucipir

	Baseline				Longitudinal			
ROI	Est (95% CI)	Cutoff[a]	Sens	Spec	Est (95% CI)	Cutoff[a]	Sens	Spec
FTLD meta-ROI	0.66 (0.56–0.75)	>1.20	62%	62%	0.68 (0.52–0.80)	>0.01	65%	67%
Midbrain	0.70 (0.59–0.79)	>1.18	60%	60%	0.68 (0.52–0.80)	>0.00	65%	67%
Pallidum	0.66 (0.56–0.75)	>1.54	62%	62%	0.53 (0.37–0.68)	>0.01	57%	56%
AD meta-ROI	0.94 (0.87–0.97)	<1.26	88%	88%	0.73 (0.57–0.84)	<0.02	65%	67%
Entorhinal cortex	0.93 (0.86–0.97)	<1.28	88%	88%	0.54 (0.38–0.69)	<0.01	57%	56%
Temporal inf	0.94 (0.87–0.97)	<1.34	87%	86%	0.70 (0.54–0.82)	<0.02	61%	63%
Orbitofrontal	0.76 (0.66–0.84)	<1.23	69%	69%	0.67 (0.51–0.80)	<0.01	61%	63%
Precentral	0.61 (0.50–0.70)	<1.13	54%	53%	0.74 (0.58–0.85)	<0.02	65%	67%
Medial parietal	0.86 (0.77–0.91)	<1.21	77%	78%	0.62 (0.46–0.75)	<0.01	61%	59%
Midbrain/temporal inf	0.99 (0.94–1.00)	>0.89	94%	95%	0.74 (0.58–0.85)	> −0.01	65%	67%
FTLD/AD meta-ROI	0.97 (0.92–0.99)	>0.96	92%	91%	0.77 (0.61–0.87)	> −0.01	65%	67%

[a]For baseline measures, the cutoff is the SUVR; for longitudinal measures, the cutoff is log(SUVR)/number of years between scans.
AD = Alzheimer disease; ADNC = AD neuropathological changes; AUROC = area under the receiver operating curve; CI = confidence interval; Est = estimate; FTLD = frontotemporal lobar degeneration; inf = inferior; ROI = region of interest; Sens = sensitivity; Spec = specificity; SUVR = standard uptake value ratio.

TABLE 5. AUROC, Sensitivity, and Specificity Data Comparing FTLD and Low ADNC Using Baseline and Rates of Change in Flortaucipir

	Baseline				Longitudinal			
ROI	Est (95% CI)	Cutoff[a]	Sens	Spec	Est (95% CI)	Cutoff[a]	Sens	Spec
FTLD meta-ROI	0.77 (0.65–0.85)	>1.18	69%	70%	0.76 (0.56–0.89)	>0.01	65%	67%
Midbrain	0.79 (0.67–0.87)	>1.16	67%	67%	0.65 (0.45–0.80)	>0.01	65%	67%
Pallidum	0.71 (0.58–0.80)	>1.51	63%	64%	0.66 (0.46–0.81)	>0.01	65%	67%
AD meta-ROI	0.52 (0.40–0.64)	>1.18	52%	52%	0.55 (0.36–0.73)	<0.00	52%	50%
Entorhinal cortex	0.50 (0.38–0.62)	<1.09	54%	55%	0.58 (0.38–0.75)	<0.01	65%	67%
Temporal inf	0.54 (0.41–0.66)	>1.22	50%	48%	0.54 (0.34–0.72)	<0.00	52%	50%
Orbitofrontal	0.68 (0.55–0.78)	>1.15	63%	64%	0.51 (0.32–0.69)	<0.01	57%	58%
Precentral	0.76 (0.64–0.85)	>1.08	67%	67%	0.57 (0.38–0.75)	>0.01	52%	50%
Medial parietal	0.54 (0.41–0.66)	>1.14	54%	55%	0.58 (0.38–0.75)	<0.01	52%	50%
Midbrain/temporal inf	0.80 (0.68–0.88)	>0.96	71%	70%	0.57 (0.37–0.74)	>0.00	57%	58%
FTLD/AD meta-ROI	0.79 (0.67–0.87)	>1.01	75%	76%	0.69 (0.48–0.83)	>−0.00	61%	58%

[a]For baseline measures, the cutoff is the SUVR; for longitudinal measures, the cutoff is log(SUVR)/number of years between scans.
AD = Alzheimer disease; ADNC = AD neuropathological changes; AUROC = area under the receiver operating curve; CI = confidence interval; Est = estimate; FTLD = frontotemporal lobar degeneration; inf = inferior; ROI = region of interest; Sens = sensitivity; Spec = specificity; SUVR = standard uptake value ratio.

TABLE 6. AUROC, Sensitivity, and Specificity Data Comparing High ADNC and Low ADNC Using Baseline and Rates of Change in Flortaucipir

	Baseline				Longitudinal			
ROI	Est (95% CI)	Cutoff[a]	Sens	Spec	Est (95% CI)	Cutoff[a]	Sens	Spec
FTLD meta-ROI	0.61 (0.48–0.72)	>1.16	57%	58%	0.61 (0.41–0.77)	>0.00	52%	50%
Midbrain	0.63 (0.51–0.74)	>1.13	57%	58%	0.51 (0.33–0.69)	>0.00	52%	50%
Pallidum	0.54 (0.42–0.66)	>1.46	48%	48%	0.67 (0.47–0.81)	>0.01	67%	67%
AD meta-ROI	0.93 (0.85–0.97)	>1.31	81%	82%	0.76 (0.57–0.88)	>0.02	74%	75%
Entorhinal cortex	0.94 (0.85–0.97)	>1.30	88%	88%	0.52 (0.33–0.70)	>0.02	48%	50%
Temporal inf	0.93 (0.85–0.97)	>1.35	84%	85%	0.72 (0.52–0.85)	>0.02	70%	67%
Orbitofrontal	0.84 (0.74–0.91)	>1.22	78%	79%	0.69 (0.49–0.83)	>0.01	63%	67%
Precentral	0.80 (0.69–0.88)	>1.09	72%	73%	0.84 (0.65–0.93)	>0.01	70%	67%
Medial parietal	0.86 (0.75–0.92)	>1.26	72%	73%	0.54 (0.35–0.72)	>0.02	59%	58%
Midbrain/temporal inf	0.94 (0.86–0.98)	<0.83	86%	85%	0.70 (0.50–0.84)	<−0.02	67%	67%
FTLD/AD meta-ROI	0.92 (0.84–0.96)	<0.89	86%	85%	0.63 (0.43–0.79)	<−0.01	59%	58%

[a]For baseline measures, the cutoff is the SUVR; for longitudinal measures, the cutoff is log(SUVR)/number of years between scans.

AD = Alzheimer disease; ADNC = AD neuropathological changes; AUROC = area under the receiver operating curve; CI = confidence interval; Est = estimate; FTLD = frontotemporal lobar degeneration; inf = inferior; ROI = region of interest; Sens = sensitivity; Spec = specificity; SUVR = standard uptake value ratio.

progressive tau accumulation is occurring across these regions in both groups. It is also worth noting that although no other FTLD ROI reached significance for longitudinal change, there was a trend for the FTLD meta-ROI to have higher accumulation rates in FTLD compared to high ADNC, which supports the FTLD meta-ROI being able to detect meaningful change over time. It is very likely that not reaching significance was due to limited power of the longitudinal sample. Regardless of the explanation, flortaucipir PET is clearly better able to differentiate FTLD from ADNC cross-sectionally rather than longitudinally, which is not surprising, because cross-sectional measures of tau capture everything that happened up until the time of the baseline scan, whereas longitudinal measures capture only what happened in the following year.

Trends for regional differences in rates of accumulation in the AD-related regions were observed between the high ADNC and low ADNC groups, with greater rates of tau accumulation in high ADNC, although these differences did not reach significance. This could have been due in part to lower power with the smaller low ADNC group or less likely because of the greater relative burden of AD pathology observed in the low ADNC group compared to the amount observed in the FTLD group (Braak NFT stage = 3.0 vs 2.5). Notably, differences in longitudinal rate of accumulation were observed in the precentral cortex, with high ADNC having higher rates of tau accumulation than FTLD and low ADNC. Longitudinal rate of uptake in the precentral cortex ROI is excellent at discriminating between high ADNC and low ADNC. Only the FTLD meta-ROI as a longitudinal marker showed good, but not excellent, discriminating power to separate FTLD from low ADNC.

We created a simple ratio of midbrain-to-inferior temporal SUVR to determine whether sensitivity and specificity to differentiate FTLD from ADNC could be improved by accounting for both an FTLD- and an AD-related region. This simple ratio was determined to be the best when applied to the baseline cohort and was superior to the AD meta-ROI and all others in separating FTLD from high ADNC. Therefore, if we had to select one measure to help separate FTLD from AD, it would be a ratio of midbrain/inferior temporal ROI. Unfortunately, the ratio provided little benefit as a longitudinal measure, further confirming the superiority of baseline measures over longitudinal change in tau PET. A more complex ratio of FTLD meta-ROI/AD meta-ROI did not perform any

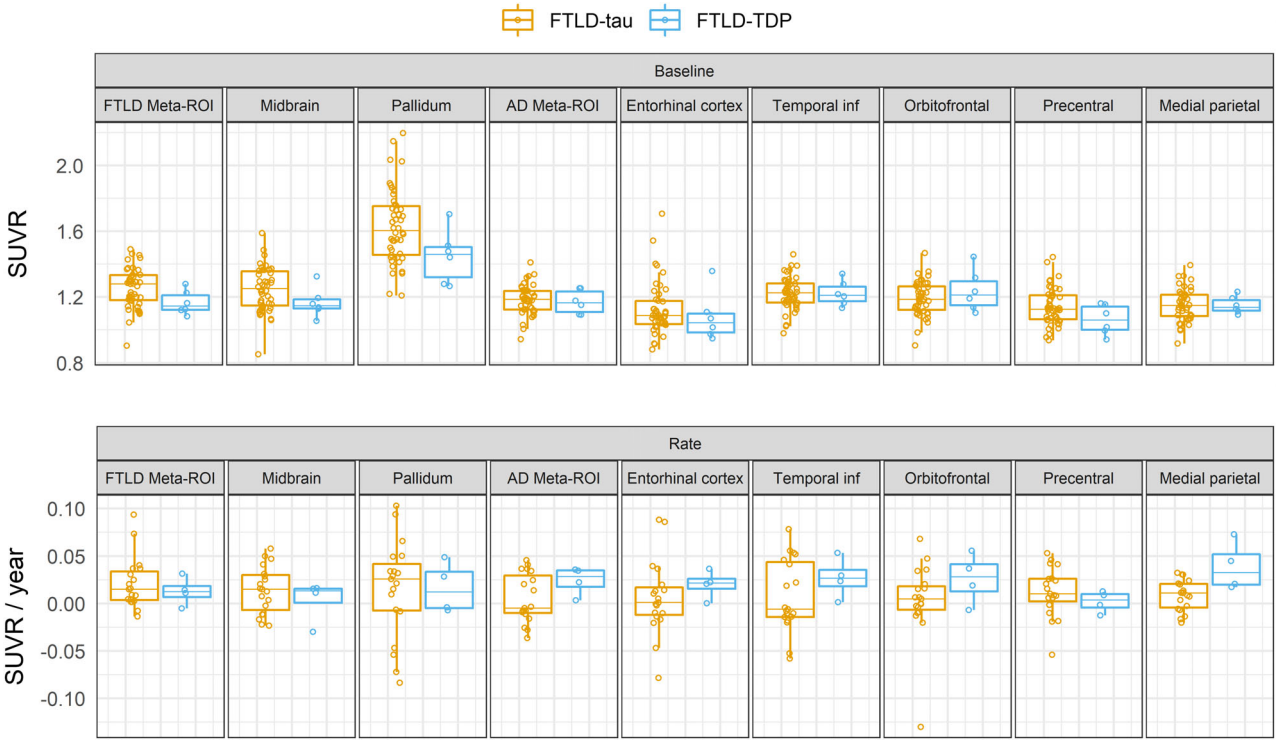

FIGURE 4: Boxplots of flortaucipir baseline and rates by frontotemporal lobar degeneration (FTLD) subtype (FTLD-tau, FTLD-TAR DNA binding protein 43 [TDP]). Individual baseline flortaucipir standard uptake value ratio (SUVR; upper) and rate of change in SUVR (lower) for each FTLD-tau and FTLD-TDP participant are shown. The upper and lower "hinges" of the boxplots correspond to the first and third quartiles (the 25th and 75th percentiles). The upper whisker extends from the hinge to the highest value that is within 1.5 × interquartile range (IQR) of the hinge, or distance between the first and third quartiles. The lower whisker extends from the hinge to the lowest value within 1.5 × IQR of the hinge. Data beyond the end of the whiskers are outliers and plotted as points. AD = Alzheimer disease; inf = inferior; ROI, region of interest.

better than the simple ratio, with the exception of possibly differentiating FTLD from low ADNC.

Our FTLD cohort consisted predominantly of FTLD-tau cases, mainly with 4R tau, with only 6 participants with FTLD-TDP. Hence, our findings regarding differences between FTLD and ADNC will likely generalize better to FTLD-tau than FTLD-TDP cohorts. The results did not change when we removed these 6 FTLD-TDP participants. This is not necessarily a limitation to our study, as FTLD-tau is more commonly associated with sporadic FTLD syndromes than FTLD-TDP, where mutations in the progranulin (*GRN*) and *C9ORF72* genes account for a significant percentage of bvFTD cases with FTLD-TDP pathology. This would also explain why flortaucipir uptake in subcortical regions was found to be the most affected in cases of sporadic bvFTD.[24]

Our study was not designed to determine what is driving the elevated uptake in FTLD. Autoradiographic studies have not found strong evidence for flortaucipir binding directly to 3R tau, 4R tau, or TDP-43. Nonetheless, multiple independent studies have reported finding a correlation between flortaucipir uptake and 4R tau burden at autopsy.[23,46,47] It has also been shown that no single 4R tau lesion is driving the correlation.[48] Possible explanations for ligand uptake include binding to 3R tau, 4R tau, and TDP-43, or to a tau/TDP-43-related protein, reflecting a process related to neurodegeneration such as inflammation or iron or off-target binding. Binding to monoamine oxidase type B (MAO-B) has been raised, but recent evidence did not support MAO-B as a target.[49] It would also not be expected that MAO-B increases over time in subcortical regions of neurodegeneration.

There are several strengths of our study, including the large number of autopsy-confirmed participants who allowed us to assess the value of flortaucipir as a diagnostic tool in ADNC cases with known Braak NFT stage and beta-amyloid status. Another strength was the utilization of a leading, highly optimized pipeline designed specifically for measuring change in tau PET, rather than more typical approaches. A limitation of the study was that we did not have enough FTLD-TDP cases to statistically compare FTLD-tau and FTLD-TDP. There is also a great deal of uncertainty regarding the biological basis for flortaucipir binding in FTLD cases.

The findings from this study have implications for the clinical utility of flortaucipir PET to differentiate

FTLD from ADNC. More work is needed to better understand the variability and biological processes and mechanisms underlying longitudinal flortaucipir changes.

Acknowledgments

The work was supported by grants from the NIH (RF1-NS112153 [K.A.J., J.L.W.], R01-DC12519 [J.L.W.], R01-NS89757 [J.L.W., K.A.J.], R01-DC14942 [K.A.J.], R01 AG50603 [J.L.W.], R37-AG11378 [C.R.J.], P30 AG062677 [R.C.P.], U01-AG 006786 [R.C.P.]), the Elsie and Marvin Dekelboum Family Foundation, and the Oxley Foundation.

We thank Dr R. Rademakers and M. Baker for genetic screening; and AVID Radiopharmaceuticals for their support in supplying the AV-1451 precursor, chemistry production advice and oversight, and US Food and Drug Administration regulatory cross-filing permission and documentation needed for this work.

Authors Contributions

K.A.J., N.T., S.D.W., and J.L.W. were responsible for study concept and design. K.A.J., N.T., S.D.W., J.L.W., V.J.L., C.G.S., M.L.S., K.K., C.R.J., D.W.D., R.R.R., F.A., H.B., J.G.-R., M.M.M., R.S., B.F.B., D.T.J., V.K.R., J.A.F., and R.C.P. were responsible for acquisition and analysis of data. K.A.J., N.T., S.D.W., R.G.G., and J.L.W. contributed to drafting the text or preparing the figures.

Potential Conflicts of Interest

Nothing to report.

References

1. Xia CF, Arteaga J, Chen G, et al. [(18)F]T807, a novel tau positron emission tomography imaging agent for Alzheimer's disease. Alzheimers Dement 2013;9:666–676.
2. Lowe VJ, Curran G, Fang P, et al. An autoradiographic evaluation of AV-1451 tau PET in dementia. Acta Neuropathol Commun 2016; 4:58.
3. Marquie M, Normandin MD, Vanderburg CR, et al. Validating novel tau positron emission tomography tracer [F-18]-AV-1451 (T807) on postmortem brain tissue. Ann Neurol 2015;78:787–800.
4. Sander K, Lashley T, Gami P, et al. Characterization of tau positron emission tomography tracer [18F]AV-1451 binding to postmortem tissue in Alzheimer's disease, primary tauopathies, and other dementias. Alzheimers Dement 2016;12:1116–1124.
5. Johnson KA, Schultz A, Betensky RA, et al. Tau positron emission tomographic imaging in aging and early Alzheimer disease. Ann Neurol 2016;79:110–119.
6. Schwarz AJ, Yu P, Miller BB, et al. Regional profiles of the candidate tau PET ligand 18F-AV-1451 recapitulate key features of Braak histopathological stages. Brain 2016;139:1539–1550.
7. Lowe VJ, Lundt ES, Albertson SM, et al. Tau-positron emission tomography correlates with neuropathology findings. Alzheimers Dement 2020;16:561–571.
8. Soleimani-Meigooni DN, Iaccarino L, La Joie R, et al. 18F-flortaucipir PET to autopsy comparisons in Alzheimer's disease and other neurodegenerative diseases. Brain 2020;143:3477–3494.
9. Fleisher AS, Pontecorvo MJ, Devous MD Sr, et al. Positron emission tomography imaging with [18F]flortaucipir and postmortem assessment of Alzheimer disease neuropathologic changes. JAMA Neurol 2020;77:829–839.
10. Marquié M, Siao Tick Chong M, Antón-Fernández A, et al. [F-18]-AV-1451 binding correlates with postmortem neurofibrillary tangle Braak staging. Acta Neuropathol 2017;134:619–628.
11. Ossenkoppele R, Rabinovici GD, Smith R, et al. Discriminative accuracy of [18F]flortaucipir positron emission tomography for Alzheimer disease vs other neurodegenerative disorders. JAMA 2018;320: 1151–1162.
12. Jack CR Jr, Wiste HJ, Schwarz CG, et al. Longitudinal tau PET in ageing and Alzheimer's disease. Brain 2018;141:1517–1528.
13. Harrison TM, La Joie R, Maass A, et al. Longitudinal tau accumulation and atrophy in aging and Alzheimer disease. Ann Neurol 2019; 85:229–240.
14. Ratnavalli E, Brayne C, Dawson K, Hodges JR. The prevalence of frontotemporal dementia. Neurology 2002;58:1615–1621.
15. Josephs KA. Frontotemporal lobar degeneration. Neurol Clin 2007; 25:683–696. vi.
16. Pottier C, Ravenscroft TA, Sanchez-Contreras M, Rademakers R. Genetics of FTLD: overview and what else we can expect from genetic studies. J Neurochem 2016;138:32–53.
17. Tsai RM, Bejanin A, Lesman-Segev O, et al. (18)F-flortaucipir (AV-1451) tau PET in frontotemporal dementia syndromes. Alzheimers Res Ther 2019;11:13.
18. Whitwell JL, Lowe VJ, Tosakulwong N, et al. [(18) F]AV-1451 tau positron emission tomography in progressive supranuclear palsy. Mov Disord 2017;32:124–133.
19. Josephs KA, Martin PR, Botha H, et al. [(18) F]AV-1451 tau-PET and primary progressive aphasia. Ann Neurol 2018;83:599–611.
20. Ali F, Whitwell JL, Martin PR, et al. [(18)F] AV-1451 uptake in corticobasal syndrome: the influence of beta-amyloid and clinical presentation. J Neurol 2018;265:1079–1088.
21. Utianski RL, Whitwell JL, Schwarz CG, et al. Tau-PET imaging with [18F]AV-1451 in primary progressive apraxia of speech. Cortex 2018; 99:358–374.
22. Makaretz SJ, Quimby M, Collins J, et al. Flortaucipir tau PET imaging in semantic variant primary progressive aphasia. J Neurol Neurosurg Psychiatry 2018;89:1024–1031.
23. Schonhaut DR, McMillan CT, Spina S, et al. (18) F-flortaucipir tau positron emission tomography distinguishes established progressive supranuclear palsy from controls and Parkinson disease: a multicenter study. Ann Neurol 2017;82:622–634.
24. Cho H, Seo SW, Choi JY, et al. Predominant subcortical accumulation of (18)F-flortaucipir binding in behavioral variant frontotemporal dementia. Neurobiol Aging 2018;66:112–121.
25. Whitwell JL, Tosakulwong N, Schwarz CC, et al. Longitudinal anatomic, functional, and molecular characterization of pick disease phenotypes. Neurology 2020;95:e3190–e3202.
26. Ghirelli A, Tosakulwong N, Weigand SD, et al. Sensitivity-specificity of tau and amyloid β positron emission tomography in frontotemporal lobar degeneration. Ann Neurol 2020;88:1009–1022.
27. Passamonti L, Vazquez Rodriguez P, Hong YT, et al. 18F-AV-1451 positron emission tomography in Alzheimer's disease and progressive supranuclear palsy. Brain 2017;140:781–791.

28. Jang YK, Lyoo CH, Park S, et al. Head to head comparison of [(18)F] AV-1451 and [(18)F] THK5351 for tau imaging in Alzheimer's disease and frontotemporal dementia. Eur J Nucl Med Mol Imaging 2018; 45:432–442.

29. Montine TJ, Phelps CH, Beach TG, et al. National Institute on Aging-Alzheimer's Association guidelines for the neuropathologic assessment of Alzheimer's disease: a practical approach. Acta Neuropathol 2012;123:1–11.

30. Jones DT, Knopman DS, Graff-Radford J, et al. In vivo (18)F-AV-1451 tau PET signal in MAPT mutation carriers varies by expected tau isoforms. Neurology 2018;90:e947–e954.

31. Cairns NJ, Bigio EH, Mackenzie IR, et al. Neuropathologic diagnostic and nosologic criteria for frontotemporal lobar degeneration: consensus of the consortium for frontotemporal lobar degeneration. Acta Neuropathol 2007;114:5–22.

32. Mackenzie IR, Neumann M, Bigio EH, et al. Nomenclature for neuropathologic subtypes of frontotemporal lobar degeneration: consensus recommendations. Acta Neuropathol 2009;117:15–18.

33. Braak H, Braak E. Neuropathological stageing of Alzheimer-related changes. Acta Neuropathol 1991;82:239–259.

34. Lowe VJ, Wiste HJ, Senjem ML, et al. Widespread brain tau and its association with ageing, Braak stage and Alzheimer's dementia. Brain 2018;141:271–287.

35. Schwarz CG, Therneau TM, Weigand SD, et al. Selecting software pipelines for change in flortaucipir SUVR: balancing repeatability and group separation. Neuroimage 2021;238:118259.

36. Josephs KA, Hodges JR, Snowden JS, et al. Neuropathological background of phenotypical variability in frontotemporal dementia. Acta Neuropathol 2011;122:137–153.

37. Sintini I, Martin PR, Graff-Radford J, et al. Longitudinal tau-PET uptake and atrophy in atypical Alzheimer's disease. Neuroimage Clin 2019;23:101823.

38. Gelman A, Hill J. *Data analysis using regression and multilevel/hierarchical models*. Cambridge, UK; New York, NY: Cambridge University Press, 2007.

39. Bang J, Spina S, Miller BL. Frontotemporal dementia. Lancet 2015; 386:1672–1682.

40. Jack CR, Wiste HJ, Weigand SD, et al. Predicting future rates of tau accumulation on PET. Brain 2020;143:3136–3150.

41. Mishra S, Gordon BA, Su Y, et al. AV-1451 PET imaging of tau pathology in preclinical Alzheimer disease: defining a summary measure. Neuroimage 2017;161:171–178.

42. Chen SD, Lu JY, Li HQ, et al. Staging tau pathology with tau PET in Alzheimer's disease: a longitudinal study. Transl Psychiatry 2021; 11:483.

43. Phillips JS, FJ 4th N, Da Re F, et al. Rates of longitudinal change in (18) F-flortaucipir PET vary by brain region, cognitive impairment, and age in atypical Alzheimer's disease. Alzheimers Dement 2021; 18:1235–1247.

44. Sintini I, Graff-Radford J, Senjem ML, et al. Longitudinal neuroimaging biomarkers differ across Alzheimer's disease phenotypes. Brain 2020;143:2281–2294.

45. Lee J, Burkett BJ, Min HK, et al. The overlap index as a means of evaluating early tau-PET signal reliability. J Nucl Med 2022; (in press).

46. Josephs KA, Whitwell JL, Tacik P, et al. [18F]AV-1451 tau-PET uptake does correlate with quantitatively measured 4R-tau burden in autopsy-confirmed corticobasal degeneration. Acta Neuropathol 2016;132:931–933.

47. McMillan CT, Irwin DJ, Nasrallah I, et al. Multimodal evaluation demonstrates in vivo (18)F-AV-1451 uptake in autopsy-confirmed corticobasal degeneration. Acta Neuropathol 2016;132:935–937.

48. Josephs K, Tosakulwong N, Weigand S, et al. Relationship between (18)F-flortaucipir uptake and histologic lesion types in 4-repeat tauopathies. J Nucl Med 2021;63:931–935.

49. Hansen AK, Brooks DJ, Borghammer P. MAO-B inhibitors do not block in vivo flortaucipir([(18)F]-AV-1451) binding. Mol Imaging Biol 2018;20:356–360.